Journal of Anatomy

J. Anat. (2010) **217**, pp694–704 doi: 10.1111/j.1469-7580.2010.01312.x

Impaired sodium levels in the suprachiasmatic nucleus are associated with the formation of cardiovascular deficiency in sleep-deprived rats

Hung-Ming Chang,[1,2] Fu-Der Mai,[3] Shiou-Ling Lei[4] and Yong-Chien Ling[4]

[1]*Department of Anatomy, Faculty of Medicine, Chung Shan Medical University, Taichung, Taiwan*
[2]*Department of Pediatrics, Chung Shan Medical University Hospital, Taichung, Taiwan*
[3]*Department of Biochemistry, College of Medicine, Taipei Medical University, Taipei, Taiwan*
[4]*Department of Chemistry, National Tsing Hua University, Hsinchu, Taiwan*

Abstract

Biological rhythms are a ubiquitous feature of all higher organisms. The rhythmic center of mammals is located in the suprachiasmatic nucleus (SCN), which projects to a number of brainstem centers to exert diurnal control over many physiological processes, including cardiovascular regulation. Total sleep deprivation (TSD) is a harmful condition known to impair cardiovascular activity, but the molecular mechanisms are unknown. As the inward sodium current has long been suggested as playing an important role in driving the spontaneous firing of the SCN, the present study aimed to determine if changes in sodium expression, together with its molecular machinery (Na-K ATPase) and rhythmic activity within the SCN, would occur during TSD. Adult rats subjected to different periods of TSD were processed for time-of-flight secondary ion mass spectrometry, Na-K ATPase assay, and cytochrome oxidase (COX) (an endogenous bioenergetic marker for neuronal activity) histochemistry. Cardiovascular dysfunction was determined through analysis of heart rate and changes in mean arterial pressure. Results indicated that, in normal rats, strong sodium signals were expressed throughout the entire SCN. Enzymatic data corresponded well with spectrometric findings in which high levels of Na-K ATPase and COX were observed in this nucleus. However, following TSD, all parameters including sodium imaging, sodium intensity as well as COX activities were drastically decreased. Na-K ATPase showed an increase in responsiveness following TSD. Both heart rate and mean arterial pressure measurements indicated an exaggerated pressor effect following TSD treatment. As proper sodium levels are essential for SCN activation, reduced SCN sodium levels may interrupt the oscillatory control, which could serve as the underlying mechanism for the initiation or development of TSD-related cardiovascular deficiency.

Key words cardiovascular rhythm; cytochrome oxidase; quantitative molecular image analysis; sleep deprivation; suprachiasmatic nucleus; time-of-flight secondary ion mass spectrometry.

Introduction

Biological rhythms originate in the temporal organization of periodic and well-coordinated neuronal activity (Benca et al. 2009; Lemmer, 2009). A regulated and rhythmic schedule serves to coordinate physiological and neurological functions with predictable changes in the environment (Martino & Sole, 2009; Reddy & ÓNeill, 2010). Previous studies have indicated that the rhythmic center of mammals is located in the suprachiasmatic nucleus (SCN) (Karatsoreos & Silver, 2007; Mendoza & Challet, 2009; Yan, 2009). Electrophysiological reports have also demonstrated that the SCN acts as a multifunctional timer, responsible for the adjustment of biochemical, physiological and metabolic homeostasis (Buijs & Kalsbeek, 2001; Brown & Piggins, 2007; Kalsbeek et al. 2007). It has been reported that the SCN spreads these time signals to numerous brain regions in the diencephalon, brainstem, and spinal cord in the form of synchronized bursts of nerve impulses (for review, see Buijs, 1996). By way of this complex neurocircuitry, the SCN imposes rhythmic activation and deactivation on the release of neuroendocrine factors, glucose metabolism,

Correspondence
Dr Hung-Ming Chang, Department of Anatomy, Faculty of Medicine, Chung Shan Medical University, 110, Section 1, Chien Kuo North Road, Taichung 402, Taiwan. T: +886 4 2473 0022 ext. 11610; F: +886 4 2473 9030; E: anatomy@csmu.edu.tw

Accepted for publication *16 September 2010*
Article published online *15 October 2010*

cardiovascular control, and regulation of the sleep–wake cycle (Nagai et al. 1996; Scheer et al. 2003; Kriegsfeld & Silver, 2006; Moore, 2007). Because the SCN constitutes the most important center for encoding the neuronal output of the biological clock, exploring the molecular mechanisms underlying the rhythmic oscillation within the SCN would not only elucidate the mechanisms of natural biorhythms, but would also provide important insights into the potential therapeutic management of clinical deficiencies.

Electrophysiological evidence, accrued over the past decade, has indicated that SCN neurons express an internal pacemaker that endows and controls rhythmic regular burst firing rates (Green & Gillette, 1982; Meijer & Rietveld, 1989; Cloues & Sather, 2003; Yamaguchi et al. 2003). The spontaneous firing patterns of SCN neurons are closely associated with the rhythmic control of sleep timing and participate in the regulation of sleep-mediated cardiovascular activities (Scheer et al. 2001; Moore, 2007). Previous studies have indicated that long-term sleep deprivation depresses the electrical activity of the SCN and impairs the rhythmic control of numerous homeostatic functions (Deboer et al. 2007). Physiological reports have also demonstrated that rhythmic disruption exerts a negative effect on cardiovascular and metabolic regulation and increases the risks of cardiovascular and metabolic diseases (Martino et al. 2008; Rüger & Scheer, 2009). A slowly inactivating component of the sodium current may play an important role in the generation of rhythmic activity within the SCN (Pennartz et al. 1997; Honma et al. 2000; Kononenko et al. 2004). By rhythmically driving the membrane potential toward threshold and by influencing transmembrane sodium gradients, these inward sodium currents drive the spontaneous firing pattern of the SCN (Jackson et al. 2004). Because the sodium-mediated ionic machinery is critical for the production of spontaneous firing, preserving sodium homeostasis within individual SCN neurons is of great importance for the maintenance of regular SCN neuronal activity.

However, although the importance of inward sodium currents has been well documented, the details concerning the concentrations of sodium as well as its relative intensity in the SCN has not yet been reported. Moreover, whether sodium concentration in the SCN would be significantly altered by total sleep deprivation (TSD), leading to a stressful condition known to disrupt the cardiovascular rhythmicity, remains to be explored. Considering that alteration of sodium levels is closely correlated to neuronal activities within the SCN, the present study aimed to determine the *in-vivo* sodium concentration together with the bioenergetic status of the SCN through the use of time-of-flight secondary ion mass spectrometry (TOF-SIMS), an advanced instrument capable of quantifying ionic content (Belu et al. 2003; Brunelle & Laprévote, 2007), and cytochrome oxidase (COX) histochemistry, which acts as an endogenous metabolic marker for neuronal activity (Wong-Riley, 1989). Furthermore, in an attempt to examine whether the ionic machinery of the SCN would subsequently be changed after TSD, changes in Na-K ATPase activity (the process responsible for restoring transmembrane ion gradients) were examined. In addition, considering the fact that arterial blood pressure and heart rate (HR) are two main cardiovascular rhythms superimposed by the SCN (Shaw & Tofler, 2009), detecting changes in mean arterial pressure (MAP) and HR after various periods of TSD could be utilized as a practical means for determining the functional significance interlinking ionic alteration and clinical cardiovascular deficiency (Mai et al. 2010).

Materials and methods

Treatment of experimental animals and surgical procedure

Adult male Wistar rats (n = 90, weighing 200–250 g) obtained from the Laboratory Animal Center of the National Taiwan University were used in this study. All surgical procedures for electroencephalogram and electromyogram recordings were performed using our well-established methods as described previously (Chang et al. 2006, 2008a, 2009). Briefly, under chloral hydrate anesthesia (0.4 mL 100 g^{-1}, i.p.), all rats were restrained in a stereotaxic apparatus equipped with a heating pad. The cranium was exposed and five stainless steel screws (Small Parts Inc., Miami Lakes, FL, USA) were implanted through the skull to serve as dural electroencephalographic electrodes. The electrodes were soldered to connectors of a plug that was fixed to the skull with dental cement. For electromyogram recording, another four stainless steel wires were inserted into the nuchal musculature. At least 10 days were allowed for recovery before experiments began. The experimental animals were then divided equally into three groups. Rats in the first group (n = 30) were subjected to TSD for 1–5 days (TSD group, with n = 6 for each TSD period). The second group was housed in the same TSD apparatus but these rats were permitted to sleep (yoked control for total sleep-deprivation (TSC) group). Animals in the third group were kept in plastic cages placed beside the TSD apparatus and so served as normal untreated controls (Untreated group). During the experimental period, all rats were exposed to an automatically regulated light–dark cycle of 12:12 h (light on 07:00–19:00 hours) at a constant room temperature of 25 ± 1 °C. The animals were allowed food and water *ad libitum*. In the care and handling of all experimental animals, the Guide for the Care and Use of Laboratory Animals (1985) as stated in the United States NIH guidelines (NIH publication No. 86-23) was followed.

Sleep deprivation process and recordings

Total sleep deprivation was performed by the disc-on-water method as described in our previous studies (Chang et al. 2006, 2008a, 2009). This method was chosen because it has previously been shown to produce effective TSD in one animal without excessive physical exertion, whereas its yoked controls (TSC group) had an acceptable amount of sleep in spite of receiving the same activity (Bergmann et al. 1989). Briefly, the apparatus comprised two rectangular clear plastic chambers placed side by side. A single plastic disc, serving as a rat-carrying platform, was

built into the lower quarter of the two chambers. Beneath the disc, and extending to the chamber walls, was a rectangular tray filled with water to a depth of 5 cm. Before the experiment began, a rat to be sleep-deprived and its yoked control were placed in the TSD apparatus for at least 7 days for environmental adaptation. Sleep deprivation depended on rats' aversion to water, as rats rarely enter water spontaneously. When sleep onset was detected in the sleep-deprived rat, the disc was rotated slowly at a moderate speed of 3.5 rpm by the computerized monitoring system, forcing both rats to keep awake and walk against the direction of disc rotation to avoid being forced into the water. When the sleep-deprived rat was spontaneously awake, the disc was stationary and the yoked control rat was able to sleep. Electroencephalographic and electromyographic data were recorded on a Grass model 78 polygraph (Grass-Telefactor, West Warwick, RI, USA) and relayed to a computer for digital recording. All of the sleep deprivation procedures were further approved by the Laboratory Animal Center Authorities of the Chung Shan Medical University.

Hemodynamic measurement

Hemodynamic measurements were performed using the well-established methods described by Nagaya et al. (1999). At either 09:00 hours (day sample group) or 21:00 hours (night sample group) on the day after the end of TSD, all rats were anesthetized via injection of 7% chloral hydrate (0.4 mL kg^{-1}) and placed on a heating pad to maintain body temperature at 37 °C. The MAP was then measured by inserting a polyethylene catheter into the right femoral artery. The HR was monitored by a tachograph that was triggered by the blood pressure waves. The hemodynamic variables of the MAP were measured using a pressure transducer (model P23 ID; Gould, Glen Burnie, MD, USA) connected to a polygraph and were recorded by a thermal recorder (7758 B System; Hewlett-Packard, Palo Alto, CA, USA).

Perfusion and tissue preparation

For TOF-SIMS analysis and quantitative histochemical study, rats from all experimental groups were killed at either 09:00 or 21:00 hours on the day after the end of TSD. Firstly, the animals were deeply anesthetized with 7% chloral hydrate (0.4 mL kg^{-1}) and then perfused transcardially with 0.9% saline followed by 300 mL of 4% paraformaldehyde in 0.1 M phosphate buffer, pH 7.4. After perfusion, the forebrain segment containing the SCN was removed and kept in the same fixative for 2 h. The tissue block was then immersed in graded concentrations of sucrose buffer (10–30%) for cryoprotection at 4 °C overnight. Serial 20-μm-thick sections of the SCN were cut transversely with a cryostat (CM3050S; Leica Microsystems, Wetzlar, Germany) on the following day and were alternately placed into two wells of a cell culture plate. Sections collected in the first well were processed for TOF-SIMS analysis, and those in the second well were processed for COX histochemistry.

Time-of-flight secondary ion mass spectrometry analysis

The TOF-SIMS analysis was carried out on a TOF-SIMS IV instrument (ION-TOF GmbH, Münster, Germany) as described in our previous studies (Chang et al. 2008a; Mai et al. 2010). Tissue sections (30 sections per animal) cryostated from each experimental rat and collected in the first well were attached to silica wafers (1×1 cm) and the temperature of the sample holder was adjusted to −60 °C. The gallium (Ga^+) ion gun operated at 25 kV was used as the primary ion source (1 pA pulse current) in this study. The Ga^+ primary ion beam was scanned over an area of 500 μm^2, which included 128×128 pixels. The acquisition time for a complete image was 200 s, and charge compensation was performed by a pulsed flood gun with low-energy electrons. The vacuum of the main chamber was kept between 10^{-7} and 10^{-8} Torr. The best resolution obtained was $m/\Delta m = 7450$. Positive secondary ions flying through a reflectron mass spectrometer were detected with a microchannel plate assembly operating at 10 kV post-acceleration. As all examined tissue sections were fully fixed by transcardial perfusion with paraformaldehyde, the paraformaldehyde molecule could be a major element in the tissue matrix. With regard to this viewpoint, it is proper to use paraformaldehyde together with a set of standard peaks [like m/z 15 (CH_3^+), 27 ($C_2H_3^+$), 41 ($C_3H_5^+$) and 69 (Ga^+)] as mass calibration to ameliorate the potential matrix effect for ion spectrums (Chang et al. 2008a). The positive ion TOF-SIMS spectrum of the molecule is dominated by an intense fragment at m/z 23 that corresponded to the sodium ion.

Cytochrome oxidase histochemistry

The method of LaManna et al. (1996) was used to measure COX reactivity with slight modifications. Sections of the SCN were incubated at 4 °C overnight in a 0.1 M phosphate-buffered medium containing 0.03% cytochrome *c*, 0.05% 3,3′-diaminobenzidine, and 0.02% catalase (pH 7.4). After incubation, sections were rinsed in distilled water to terminate the reaction. Before densitometric studies, all reacted sections were mounted on gelatinized slides, dehydrated through a graded series of alcohol, cleared with xylene, and fixed onto cover slips with Permount.

Preparation of microsomes

For Na-K ATPase activity assay, microsomes were prepared from unfixed brain segments containing the SCN (Adya & Mallick, 1998). After decapitation, five rat brains from each experimental group ($n = 15$) were removed and homogenized in ice-cold buffer containing 0.32 M sucrose, 12.5 mM Tris, and 1 mM EDTA, pH 7.4. The homogenate was centrifuged for 5 min at 2935 *g*. The pellet was discarded and the supernatant was further centrifuged for 20 min at 11 740 *g* and then for 60 min at 127 850 *g*. The resulting pellet was then suspended in 5 mM EDTA, stirred for 30 min, and centrifuged at 11 740 *g* for 5 min. The supernatant fraction was brought to 30% saturation by the addition of saturated ammonium sulphate (pH 7.4) with Tris. This solution was then stirred for 30 min and further centrifuged for 30 min at 11 740 *g*. The precipitate was resuspended in 5 mM EDTA and stored at 4 °C for 10–12 h before use. Lowry's method (Lowry et al. 1951) was used for protein estimation in the microsomal sample.

Na-K ATPase activity assay

The method of Gulyani & Mallick (1993) was used to quantify Na-K ATPase activity. The reaction mixture contained 100 mM

NaCl, 20 mM KCl, 5 mM $MgCl_2$, 3 mM ATP, and 50 mM Tris, pH 7.4. An aliquot (35 μg protein) of the microsomes was incubated with the reaction mixture for 20 min at 37 °C. Adenosine triphosphate was used as the substrate and the ouabain was applied as a specific blocker of Na-K ATPase activity. The absorbance of liberated phosphate was estimated at 660 nm in a Simadzu UV260 spectrophotometer (Fiske & Subbarow, 1925). The ouabain-sensitive Na-K ATPase activity was quantified and expressed as μmol of Pi released per mg protein per hour.

Quantitative study and image analysis

The general approach for all quantitative image analyses was similar to our previous studies (Chang et al. 2005, 2008b). A total of 10–15 sections per animal, representing the entire extent of the SCN, were used. The COX staining intensity was quantified with a computer-based image analysis system (MGDS) using Image-Pro Plus software (Media Cybernetics, Silver Spring, MD, USA). A digital camera mounted on the Zeiss microscope (Axioplan 2; Carl Zeiss MicroImaging GmbH, Hamburg, Germany) imaged sections at 50 × magnification in bright-field mode and displayed them on a high-resolution monitor. The optical density (OD) of the suprachiasmatic neurons stained for COX activity was measured within the boundary of a line encircling the labeled somata on the digitized image. The recorded densitometric readings represent the OD of the pixels for that cell. A total of 50–100 neurons per section were measured. All densitometric readings taken from all suprachiasmatic neurons in each section were then combined and averaged to obtain the total OD for that section. The background OD staining of each section was measured by averaging 10 random rectangles (area of rectangle = 150 μm^2) over the image of the optic chiasm. The true OD for each section was then expressed by subtracting the background OD from total OD, so that each measurement was made in an unbiased way to correct for background. All images were captured on the same day by the same experimenter to maintain uniform camera and digitizer gain settings. As the actual amount of reaction product deposited in a tissue section from COX activity is influenced by a variety of factors, all parameters were carefully controlled following the recommended procedures for gray level adjustment, histogram stretch, and minimal OD (Smolen, 1990).

Statistical analysis

For TOF-SIMS data analysis, spectral intensities detected from each section were normalized to the ion intensity of paraformaldehyde (serve as baseline = 100%) and expressed as percentage above the baseline. All of the normalized spectra collected from each animal were then averaged to obtain the representative data for that animal. The representative data acquired from animals belonging to the same experimental group were further averaged to yield the group mean. Comparisons among the group means as well as other data acquired from enzymatic and densitometric readings for untreated, TSC, and different periods of TSD rats were subjected to one-way ANOVA analysis with repeated measures. The effect of each challenge compared with the untreated group was further analyzed using the Bonferroni *post hoc* test. The statistical difference was considered significant if $P < 0.05$.

Results

Total sleep deprivation reduced sodium in suprachiasmatic nucleus neurons

Figure 1 illustrates the TOF-SIMS positive ion mass spectra in *m/z* 23 reflecting the quantitative intensity (Fig. 1A,B) and normalized spectral intensity (Fig. 1C) of Na^+ in the SCN of normal untreated, TSC, and TSD rats. In normal untreated rats, the quantitative intensity of the major peak of Na^+ in the SCN was determined to be 9.88×10^4 (total ion counts per 500 μm^2) (Fig. 1A). However, in the TSD-treated groups, the SCN Na^+ intensity was only 4.35×10^4 (total ion counts per 500 μm^2) (Fig. 1B). Data obtained from the normalized spectral intensity also showed a lower concentration of Na^+ following 5 days of TSD (e.g. 2.734 ± 0.15% in the day sample group and 2.012 ± 0.13% in the night sample group) compared with that of normal untreated rats (7.011 ± 0.18% as well as 4.009 ± 0.17% in day and night sample groups, respectively) (Fig. 1C). It is noteworthy that, regardless of the sample time-point, the reduction in Na^+ intensity in the SCN after TSD was a universal pattern proportional to the duration of TSD (Fig. 1C).

Time-of-flight secondary ion mass spectrometry Na^+ imaging of individual neurons

The distribution of Na^+ within the SCN was examined by TOF-SIMS imaging in brain sections from TSD-treated and untreated control rats. Analysis revealed that Na^+ signals were distributed throughout the SCN with clearly defined profiles (Fig. 2A). The specific pattern of ionic distribution indicated that most Na^+ was localized to the intracellular portion of the SCN neurons (Fig. 2A). However, in rats subjected to various periods of TSD, the Na^+ signal within SCN neurons was significantly lower (Fig. 2B–F). The reduction of Na^+ was detected as early as 1 day into TSD treatment (Fig. 2B), and reached a nadir at day 5 (Fig. 2D,F). It should be noted that a reduction in Na^+ was observed in both day and night sample groups (Fig. 2C–F), suggesting that the reduced Na^+ signal was a specific effect resulting from TSD treatment.

Cytochrome oxidase histochemical reaction and quantitative image analysis

In normal untreated rats, numerous COX-reactive neurons with moderate to strong staining intensities were observed in the SCN (Fig. 3A,B). The COX-reactive neurons were scattered throughout the SCN without specific distribution patterns (Fig. 3A,B). Both the distribution pattern and staining intensity of COX-reactive neurons were similar between TSC and normal untreated rats. However, in the TSD-treated group, the staining intensity of COX-reactive neurons was drastically decreased (Fig. 3C,D). Only a few cells with weak or moderate staining intensity were detected in the SCN

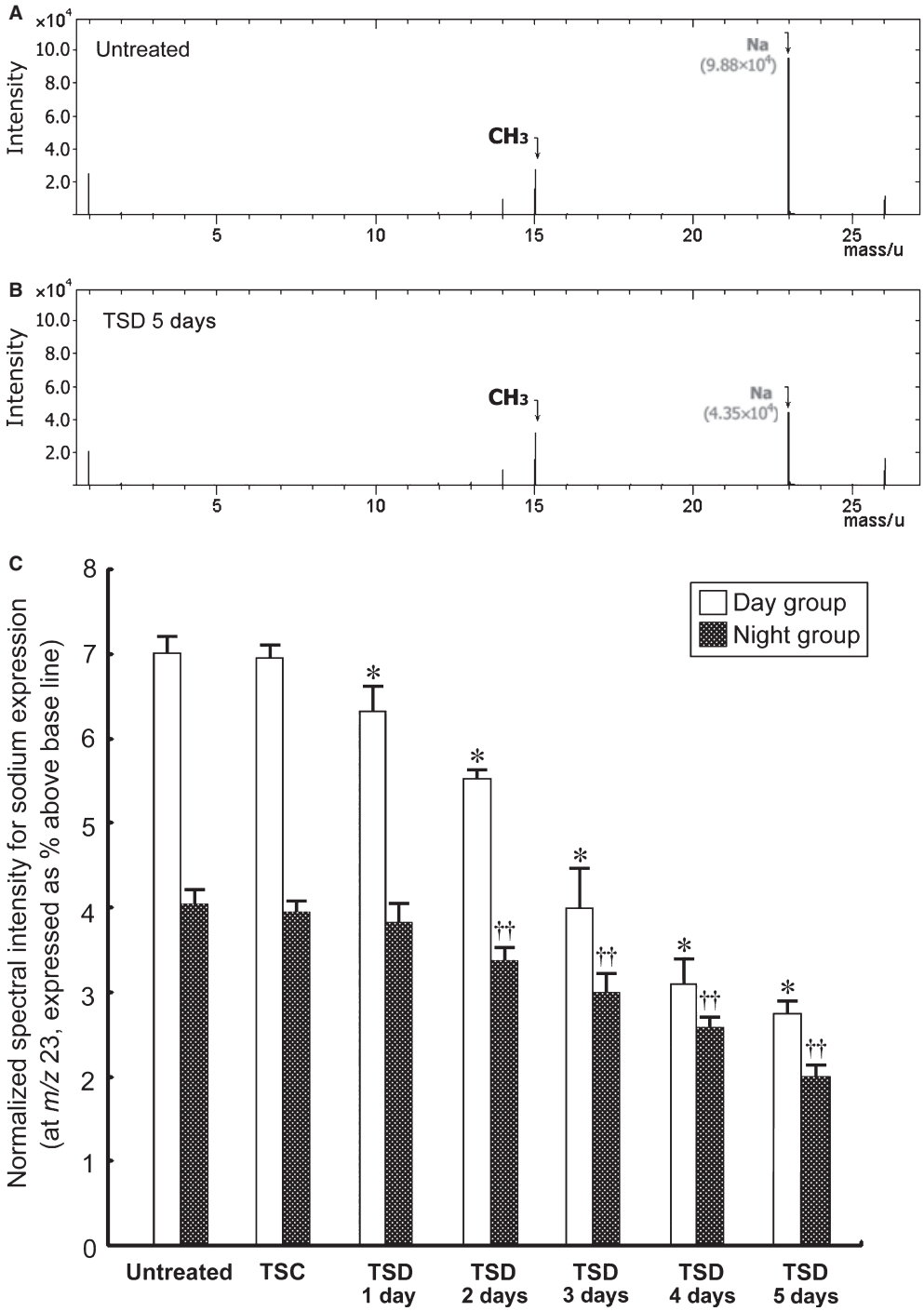

Fig. 1 Time-of-flight secondary ion mass spectrometry positive ion spectrum (A,B) and histogram (C) showing quantitative intensity (total ion counts per 500 μm^2) and normalized spectral intensity of Na^+ (expressed as percentage above the baseline) in the suprachiasmatic nucleus of normal untreated, control for total sleep-deprived (TSC) and total sleep-deprived (TSD) rats. In normal untreated rats (A), the quantitative intensity of Na^+ was 9.88×10^4 (total ion counts per 500 μm^2). However, following 5 days of TSD (B), the Na^+ intensity was much lower (4.35×10^4; total ion counts per 500 μm^2). Similar findings were observed in the normalized spectral intensity (C), in which data obtained from untreated rats (7.011 ± 0.18% for the day group and 4.003 ± 0.16% for the night group) were significantly higher than from TSD rats (2.734 ± 0.15% for the day group and 2.112 ± 0.22% for the night group following 5 days of TSD). It is noteworthy that, no matter at which time-point the sample was performed (day or night group), the normalized spectral intensity showed a decrease in the expression after TSD treatment. *$P < 0.05$ compared with the day group of normal untreated rats; ††$P < 0.05$ compared with the night group of normal untreated rats.

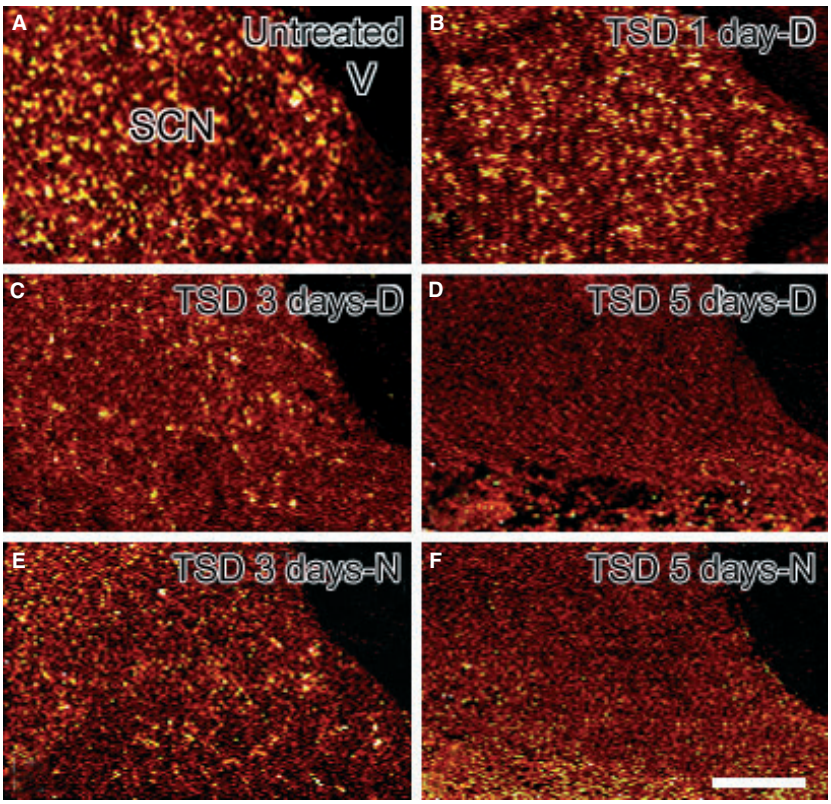

Fig. 2 Time-of-flight secondary ion mass spectrometry positive ion image showing Na^+ expression in the suprachiasmatic nucleus (SCN) of normal untreated (A) and total sleep-deprived rats (TSD) with different duration and sample time-points (B–F). The molecular imaging of Na^+ signals is expressed by a color scale in which bright colors represent high levels of Na^+. In normal untreated rats (A), many neurons in the SCN exhibited strong Na^+ signals. However, following various periods of TSD (B–F), the ionic image of Na^+ was decreased in intensity, with the maximal change observed in animals subjected to 5 days of TSD (D,F). It is noteworthy that the reduction of the Na^+ signal in the SCN following TSD was similar in both the day (D) and night (N) sample groups (C vs. E and D vs. F). V, third ventricle. Scale bar = 150 μm.

following TSD (Fig. 3C,D). The reduced expression of COX reactivity was evident in both day and night sample groups (Figs 3C,D and 4). Quantitative image analysis revealed that the true OD of COX reactivity had gradually decreased from 1.89 ± 0.06 in the day sample group of normal untreated rats to 0.97 ± 0.04 in the corresponding group of rats after 5 days of TSD (Fig. 4). Similar findings were observed in the night sample group in which a significant decrease of COX reactivity was detected in rats subjected to various periods of TSD treatment (e.g. from 1.62 ± 0.07 to 0.69 ± 0.02 in night sample groups of normal untreated and 5 days of TSD rats, respectively) (Fig. 4).

Total sleep deprivation increased Na-K ATPase activity

As shown in Fig. 5, there was no significant difference in Na-K ATPase activity between normal untreated and TSC-treated rats. However, following various periods of TSD, a considerable increase in Na-K ATPase activity was observed in the SCN as compared with that of normal untreated rats (Fig. 5). Spectrophotometric data revealed that the Na-K ATPase activity had significantly increased from 12 ± 0.58 μM Pi released per mg protein per h in the day sample group of normal untreated rats to 22 ± 0.79 μM Pi released per mg protein per h in the corresponding group of rats following 5 days of TSD (Fig. 5). Consistent with the spectrometric and histochemical results, no significant difference in Na-K ATPase activity was detected between the day sample and night sample groups following TSD treatment (Fig. 5).

Heart rate and mean arterial pressure were increased by total sleep deprivation

The changes in HR and MAP in each experimental group (normal untreated, TSC, and TSD) were expressed by averaging the data collected from both day and night sample groups (Fig. 6). In normal untreated and TSC rats, MAP was estimated to be 120 ± 4.7 and 118 ± 3.9 mmHg, respectively (Fig. 6A). However, following 5 days of TSD, MAP increased significantly to nearly 157 ± 7.8 mmHg (Fig. 6A). Similar findings were observed in HR measurements in which an enhanced effect (from 402 ± 6 beats min^{-1} in normal untreated rats to 463 ± 3 beats min^{-1} in 5 days of TSD rats) was detected in all TSD groups (Fig. 6B). These results indicated that TSD had induced cardiovascular dysfunction, which might have been caused by the depressed activation of the SCN originating from impaired concentrations of Na^+.

Discussion

This research represents the first study employing quantitative spectrometric and molecular imaging analysis to clearly demonstrate that *in-vivo* Na^+ concentrations were

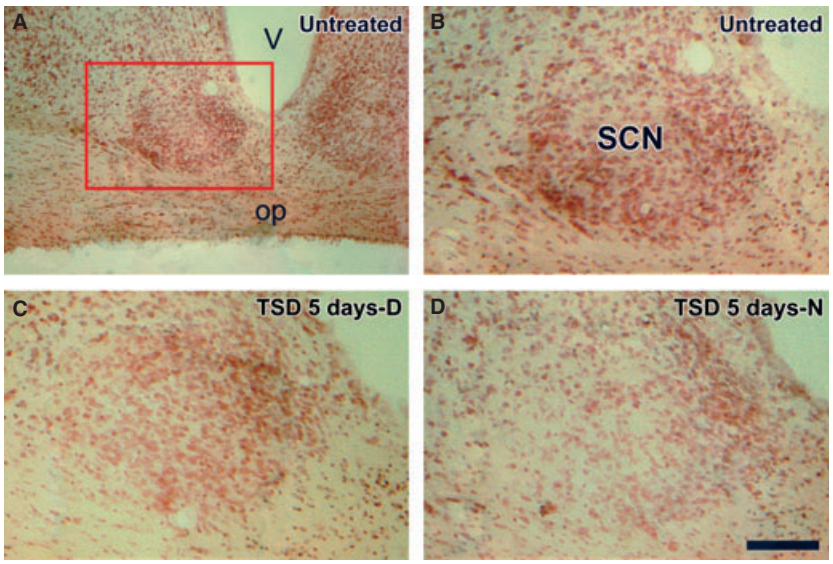

Fig. 3 Lower (A) and higher (B–D) magnification of light photomicrographs showing cytochrome oxidase (COX) reactivity in the suprachiasmatic nucleus (SCN) of normal untreated (A,B) and total sleep-deprived (C,D) rats. In normal untreated rats (A,B), numerous moderate to strong COX-reactive neurons were identified in the SCN. However, following 5 days of total sleep deprivation (TSD) (C,D), only a few neurons with weak COX staining intensity were detected (C,D). Also note that the reduction of COX expression was evident in both groups at different sample time-points (C,D). D, day; N, night; V, third ventricle; op, optic chiasma; Scale bar = 400 μm in (A) and 200 μm in (B–D).

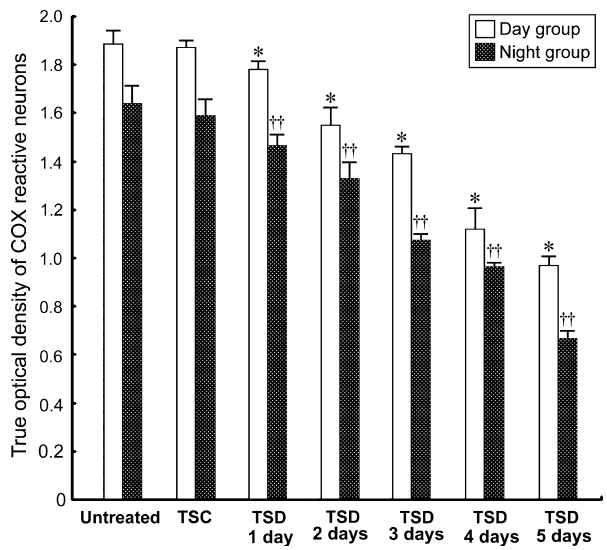

Fig. 4 Histogram showing quantitative cytochrome oxidase (COX) staining intensity [expressed as true optical density (OD)] in the suprachiasmatic nucleus (SCN) of normal untreated control for total sleep-deprived (TSC) and total sleep-deprived rats (TSD) with different sample time-points. In normal untreated and TSC rats, numerous COX-reactive neurons with high true OD were detected in the SCN. In contrast, the staining intensity of COX in the SCN decreased progressively over the duration of TSD. Decreasing COX reactivity was apparent in both the day and night sample groups. *$P < 0.05$ as compared with the day group of normal untreated rats; ††$P < 0.05$ as compared with the night group of normal untreated rats.

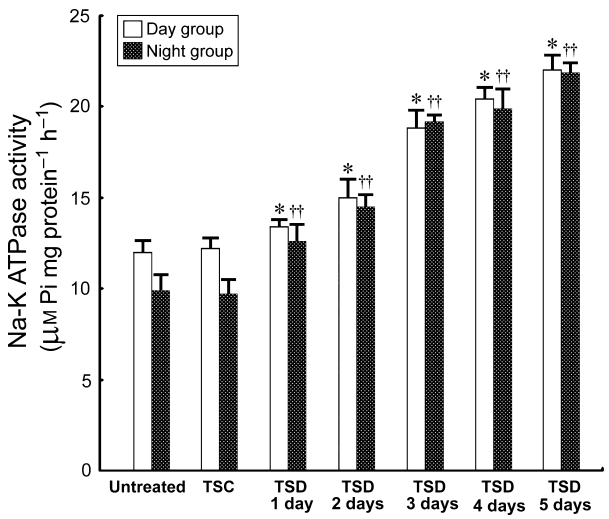

Fig. 5 Histogram showing the Na-K ATPase activity in the suprachiasmatic nucleus (SCN) of normal untreated control for total sleep-deprived (TSC) and total sleep-deprived (TSD) rats with different sample time-points. Note that the Na-K ATPase activity of the SCN had significantly increased with extension of TSD. Also note that, even among samples at different time-points (day or night group), up-regulation of Na-K ATPase activity was clearly observable in both groups following TSD treatment. *$P < 0.05$ compared with the day group of normal untreated rats; ††$P < 0.05$ compared with the night group of normal untreated rats.

significantly decreased in the SCN by TSD (Figs 1 and 2). The reduction in Na^+ concentration was evident after 1 day of TSD (Figs 1C and 2B) and reached its nadir after 5 days (Figs 1C and 2D,F). It has been well established that the SCN functions as the mammalian central biological clock, and that spontaneous firing rates coordinate peripheral oscillators to control a wide variety of biochemical, physiological, and behavioral rhythms (Karatsoreos & Silver, 2007; Mendoza & Challet, 2009; Yan, 2009). The slowly inactivating component of the inward sodium current may play an important role in driving the spontaneous firing of the SCN (Pennartz et al. 1997; Jackson et al. 2004; Kononenko et al. 2004). The transmembrane Na^+ gradient is determined mainly by Na^+ influx through sodium channels and egress by Na-K ATPase activity. In turn, the Na^+ gradient

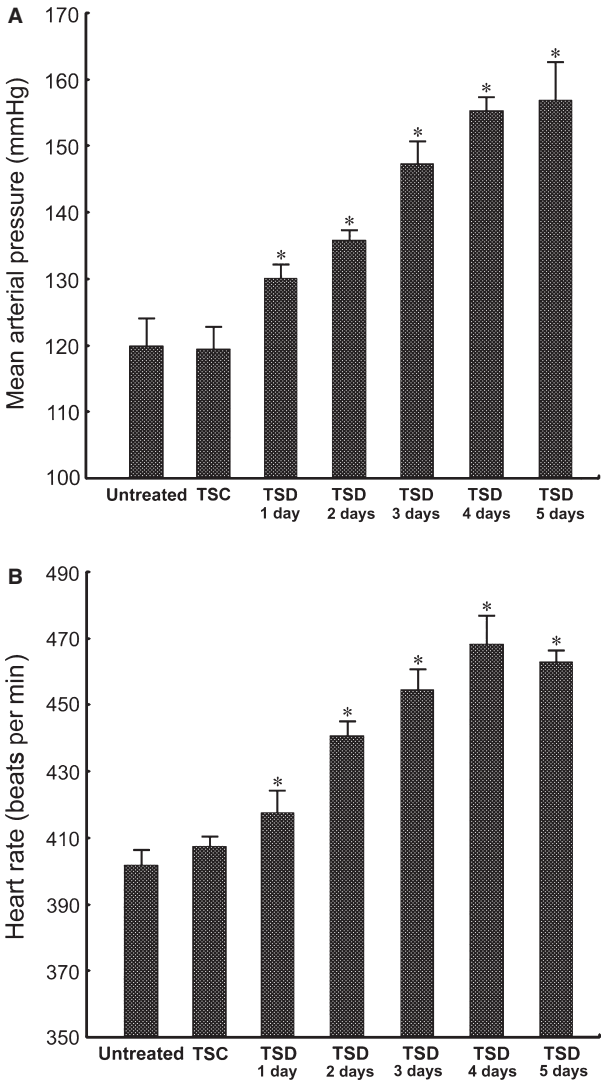

Fig. 6 Histograms showing the mean arterial pressure (MAP) (A) and heart rate (HR) (B) of normal untreated, control for total sleep-deprived (TSC) and total sleep-deprived (TSD) rats. Data are expressed as the averaged value detected from both the day and night groups. In normal untreated rats, MAP and HR were 120 ± 4.7 mmHg and 402 ± 6 beats min^{-1}. In the TSC group, MAP and HR were 118 ± 3.9 mmHg and 407 ± 2 beats min^{-1}. In rats treated with TSD for 5 days, however, both MAP and HR were considerably elevated to 157 ± 7.8 mmHg and 463 ± 3 beats min^{-1}, respectively, indicating a deficiency in cardiovascular regulation. $*P < 0.05$ as compared with normal untreated values.

determines action potential magnitude and the rate of depolarization mediated by slow inward sodium currents in SCN neurons (Pennartz et al. 1997; Jackson et al. 2004). Hence, maintaining Na^+ homeostasis is vital for maintaining proper firing patterns in both SCN neurons and in follower brainstem neurons that control cardiac and vascular parameters like HR and blood pressure. From this point of view, reduced concentrations of intracellular Na^+, possibly concomitant with increased Na-K ATPase activity, could markedly disrupt the ionic machinery responsible for neuronal firing, leading to the dysfunction of the medullar rhythmic control center and cardiovascular deficiency. Such is the case in this study, where we clearly detected a decrease in COX reactivity (Fig. 4) and elevated Na-K ATPase activity (Fig. 5) in the SCN of rat subjected to the stress of TSD. The alteration of these Na^+-related elements following TSD could contribute to the emergence of irregular cardiovascular rhythmicity (Fig. 6). It was suggested that COX is a bioenergetic enzyme involved in the generation of ATP; thus, COX activity may be critical for maintaining the membrane potential, which is the ultimate shaper of neuronal patterns (Deyoe et al. 1995). Indeed, changes in COX reactivity have been well documented to cause changes in neuronal firing (Mawe & Gershon, 1986; Adret & Margoliash, 2002). Because COX expression was noticeably decreased in the SCN following TSD (Fig. 4), it is reasonable to expect that SCN activation and output would change. Considering that the SCN sends output signals to numerous cardiovascular control regions, this study strongly suggests that the cardiovascular dysfunction observed after TSD resulted from impaired SCN activation due to impaired sodium levels that disrupted normal inputs to brainstem centers.

Although the importance of maintaining the Na^+ gradient for control of SCN neuron rhythmic firing has been well documented, other ionic mechanisms cannot be discounted. Previous studies have indicated that both K^+ and L-type Ca^{2+} currents shape the spontaneous firing patterns of SCN neurons (Pennartz et al. 2002; Belle et al. 2009). Electrophysiological reports also demonstrated that Ca^{2+} currents mediate the rising phase of burst firing, and thereby provided an excitatory drive for neuronal activation, whereas the falling phase was mediated by K^+ currents that in turn determined the deactivation kinetics of Na^+ channels (Pennartz et al. 2002; Schaap et al. 2003). Hence, these particular ionic conductors could play a central role in circadian firing and exert a major influence on the bioelectrical output of the SCN neurons (Belle et al. 2009). In addition, by significantly altering the intracellular ionic homeostasis, periodic entry of Ca^{2+} or Na^+ might regulate the kinase cascades involved in gene expression or neuronal plasticity, leading to long-term changes in SCN function (Dolmetsch et al. 1998; Cantrell & Catterall, 2001).

Aside from the diurnal changes in ionic currents, the intracellular molecular clock incorporated in each SCN neuron has been demonstrated to exert divergent effects on multiple ion channels, which may act in concert to generate coordinated and rhythmic firing activity (Reppert & Weaver, 2001). However, caution must be exercised when interpreting how changing individual ion channels or pumps following TSD would alter the firing of neurons within the SCN, as the spatiotemporal interaction between ionic concentration and the activation of the SCN is slightly more complex than had previously been supposed.

Proper maintenance of Na^+ depends on sodium pump activity (Therien & Blostein, 2000; Kaplan, 2002). We surmised that challenges to normal SCN function, as imposed by TSD, would change this ionic machinery. Previous studies have reported that Na-K ATPase activation contributes to rhythmic generation in cultured spinal networks and neurons within the SCN (Darbon et al. 2003; Wang & Huang, 2006). Pharmacological reports have also demonstrated that rapid eye movement sleep deprivation could augment Na-K ATPase activity, thereby causing changes in the excitability of SCN neurons (Gulyani & Mallick, 1993). It has been suggested that the efficiency of synaptic transmission could be modulated by the stimulation or inhibition of Na-K ATPase activity (Phillis, 1992). Stimulation of this sodium pump could lead to hyperpolarization, which would depress spontaneous firing (Phillis, 1992). Conversely, inhibition of this sodium pump would initiate depolarization and enhance the excitability of the neurons (Phillis, 1992). This viewpoint is in good agreement with our present study, in which we successfully detected an elevation in Na-K ATPase activity in the SCN following TSD (Fig. 5). The increase in Na-K ATPase activity was accompanied by a depression of neuronal activation, as revealed by the decrease in COX reactivity (Fig. 4). As the neuronal activation of the SCN is regulated by Na^+ current modulated next to the activity of Na-K ATPase (Wang & Huang, 2006), increased Na-K ATPase activity of the SCN following TSD may constitute a compensatory attempt to counteract the greater dissipation of Na^+ gradients. This counter-reaction may over-excite the electrogenic nature of this enzyme and, consequently, lead to the reduced firing in the SCN that interrupts the oscillatory control of the SCN to downstream cardiovascular regulating regions.

Recent findings have reported that sleep deprivation could reset the circadian clock and alter gene expression, without substantial locomotor activity (Antle & Mistlberger, 2000). Therefore, we examined two sample time-points (09:00 and 21:00 hours) to elucidate whether any phase-shift existed following various periods of TSD. In our results, normal untreated rats showed significant differences in Na^+ signals between the two sample groups, with higher levels observed in daytime-sampled animals (Fig. 1C). Similar findings were also observed in histochemical and biochemical reactions, in which higher levels of COX staining and Na-K ATPase activity were observed in the daytime-sampled animals (Figs 4 and 5). The enhanced SCN Na^+ expression in the daytime was clearly associated with increased COX reactivity, representing strong diurnal oscillations of SCN activity. However, in animals subjected to differing periods of TSD, the Na^+ concentration, COX activity, and Na-K ATPase activity did not show significant differences between the two sample groups (Figs 1C, 4 and 5). Data collected from daytime samples were very similar to those obtained from night-time samples (Figs 1C, 4 and 5). These results indicated that there was no noticeable phase-shift associated with TSD treatment. Although the detailed mechanism responsible for the parallel expression between two sample groups following TSD is not fully understood, the intensity of TSD (up to 5 days) as well as the state of arousal at waking may account for the discrepancies between our results and those reported in previous studies (with TSD merely lasting for a few hours). Indeed, the magnitude of the phase-shift has already been reported to be inversely related to the awaking status of the sleep-deprived animals (Antle & Mistlberger, 2000).

Another issue to be addressed is that, although TSD is a well-established model widely used in clinical research, it remains debatable whether any of the results obtained from this regime could be directly attributed to TSD. Because our TSD paradigm was based on the disc-on-water method, any possible effect (e.g. increases in physical activity) that might affect neuronal activity or cardiovascular function should not be overlooked. With this in mind, we used the yoked control (TSC group) to serve as an internal control for TSD to evaluate possible changes in these parameters (Chang et al. 2008b, 2009). Results obtained in this study revealed that data collected from the TSC group were very similar to those observed in the untreated group in spectrometric, biochemical, histochemical or hemodynamic measurements (Figs 1C, 4, 5 and 6). Given that TSC rats had performed the same physical activities and had been treated in precisely the same manner as the TSD rats, the marked discrepancies detected between the two groups suggest that these alterations were due specifically to a lack of sleep, and not to the minor influences of physical debilitation produced in the current experimental paradigm.

Conclusion

With the coming of industrialization, chronic sleep loss or sleep deprivation is becoming an important threat to overall health. Although the mechanisms responsible for development of TSD-induced cardiovascular dysfunction are not yet fully understood, through a powerful combination of molecular, spectrometric, biochemical, and morphological approaches, the present study indicates a role for impaired Na^+ levels in the development of TSD-related cardiovascular deficiencies. Because the inward Na^+ current may serve as the primary pacemaker in the SCN, impaired Na^+ levels following TSD could disrupt activity within the SCN. Through intensive neuronal networks interlinking the output of the SCN to several regions of rhythmic generation, decreases in the activation of the SCN could depress the oscillatory control, consequently leading to the initiation or development of TSD-relevant cardiovascular disability.

Acknowledgements

This study was supported in part by research grants (NSC 97-2320-B040-011 and NSC 98-2320-B040-007) to H.-M.C. from the

National Science Council, Taiwan. The authors confirm that there are no known conflicts of interest associated with this research and there has been no significant financial support for this work that could have influenced its outcome.

References

Adret P, Margoliash D (2002) Metabolic and neural activity in the song system nucleus robustus archistriatalis: effect of age and gender. *J Comp Neurol* **454**, 409–423.

Adya HVA, Mallick BN (1998) Comparison of Na-K ATPase in the rat brain synaptosome under different conditions. *Neurochem Int* **33**, 283–286.

Antle MC, Mistlberger RE (2000) Circadian clock resetting by sleep deprivation without exercise in the Syrian hamster. *J Neurosci* **20**, 9326–9332.

Belle MDC, Diekman CO, Forger DB, et al. (2009) Daily electrical silencing in the mammalian circadian clock. *Science* **326**, 281–284.

Belu AM, Graham DJ, Castner DG (2003) Time-of-flight secondary ion mass spectrometry: techniques and applications for the characterization of biomaterial surfaces. *Biomaterials* **24**, 3635–3653.

Benca R, Duncan MJ, Frank E, et al. (2009) Biological rhythms, higher brain function, and behavior: gaps, opportunities, and challenges. *Brain Res Rev* **62**, 57–70.

Bergmann BM, Kushida CA, Everson CA, et al. (1989) Sleep deprivation in the rat: II. Methodology. *Sleep* **12**, 5–12.

Brown TM, Piggins HD (2007) Electrophysiology of the suprachiasmatic circadian clock. *Prog Neurobiol* **82**, 229–255.

Brunelle A, Laprévote O (2007) Recent advances in biological tissue imaging with Time-of-flight Secondary Ion Mass Spectrometry: polyatomic ion sources, sample preparation, and applications. *Curr Pharm Des* **13**, 3335–3343.

Buijs RM (1996) The anatomical basis for the expression of circadian rhythms: the efferent projections of the suprachiasmatic nucleus. *Prog Brain Res* **111**, 229–240.

Buijs RM, Kalsbeek A (2001) Hypothalamic integration of central and peripheral clocks. *Nat Rev Neurosci* **2**, 521–526.

Cantrell AR, Catterall WA (2001) Neuromodulation of Na^+ channels: an unexpected form of cellular plasticity. *Nat Rev Neurosci* **2**, 397–407.

Chang HM, Tseng CY, Wei IH, et al. (2005) Melatonin restores the cytochrome oxidase reactivity in the nodose ganglia of acute hypoxic rats. *J Pineal Res* **39**, 206–214.

Chang HM, Wu UI, Lin TB, et al. (2006) Total sleep deprivation inhibits the neuronal nitric oxide synthase and cytochrome oxidase reactivities in the nodose ganglion of adult rats. *J Anat* **209**, 239–250.

Chang HM, Mai FD, Chen BJ, et al. (2008a) Sleep deprivation predisposes liver to oxidative stress and phospholipid damage – a quantitative molecular imaging study. *J Anat* **212**, 295–305.

Chang HM, Huang YL, Lan CT, et al. (2008b) Melatonin preserves superoxide dismutase activity in hypoglossal motoneurons of adult rats following peripheral nerve injury. *J Pineal Res* **44**, 172–180.

Chang HM, Wu UI, Lan CT (2009) Melatonin preserves longevity protein (sirtuin 1) expression in the hippocampus of total sleep-deprived rats. *J Pineal Res* **47**, 211–220.

Cloues RK, Sather WA (2003) After hyperpolarization regulates firing rate in neurons of the suprachiasmatic nucleus. *J Neurosci* **23**, 1593–1604.

Darbon P, Tscherter A, Yvon C, et al. (2003) Role of the electrogenic Na/K pump in disinhibition-induced bursting in cultured spinal networks. *J Neurophysiol* **90**, 3119–3129.

Deboer T, Détári L, Meijer JH (2007) Long term effects of sleep deprivation on the mammalian circadian pacemaker. *Sleep* **30**, 257–262.

Deyoe EA, Trusk TC, Wong-Riley MT (1995) Activity correlates of cytochrome oxidase-defined compartments in granular and supragranular layers of primary visual cortex of the macaque monkey. *Vis Neurosci* **12**, 629–639.

Dolmetsch RE, Xu K, Lewis RS (1998) Calcium oscillations increase the efficiency and specificity of gene expression. *Nature* **392**, 933–936.

Fiske CH, Subbarow J (1925) The colorimetric determination of phosphorus. *J Biol Chem* **66**, 375–400.

Green DJ, Gillette R (1982) Circadian rhythm of firing rate recorded from single cells in the rat suprachiasmatic brain slice. *Brain Res* **245**, 198–200.

Gulyani S, Mallick BN (1993) Effect of rapid eye movement sleep deprivation on rat brain Na-K ATPase activity. *J Sleep Res* **2**, 45–50.

Honma S, Shirakawa T, Nakamura W, et al. (2000) Synaptic communication of cellular oscillations in the rat suprachiasmatic neurons. *Neurosci Lett* **294**, 113–116.

Jackson AC, Yao GL, Bean BP (2004) Mechanism of spontaneous firing in dorsomedial suprachiasmatic nucleus neurons. *J Neurosci* **24**, 7985–7998.

Kalsbeek A, Kreier F, Fliers E, et al. (2007) Minireview: circadian control of metabolism by the suprachiasmatic nuclei. *Endocrinology* **148**, 5635–5639.

Kaplan JH (2002) Biochemistry of Na-K ATPase. *Annu Rev Biochem* **71**, 511–535.

Karatsoreos IN, Silver R (2007) Minireview: the neuroendocrinology of the suprachiasmatic nucleus as a conductor of body time in mammals. *Endocrinology* **148**, 5640–5647.

Kononenko NI, Shao LR, Dudek FE (2004) Riluzole-sensitive slowly inactivating sodium current in rat suprachiasmatic nucleus neurons. *J Neurophysiol* **91**, 710–718.

Kriegsfeld LJ, Silver R (2006) The regulation of neuroendocrine function: timing is everything. *Horm Behav* **49**, 557–574.

LaManna JC, Kutina-Nelson KL, Hritz MA, et al. (1996) Decreased rat brain cytochrome oxidase activity after prolonged hypoxia. *Brain Res* **720**, 1–6.

Lemmer B (2009) Discoveries of rhythms in human biological functions: a historical review. *Chronobiol Int* **26**, 1019–1068.

Lowry OH, Rosenbrough NJ, Farr AL, et al. (1951) Protein measurement with Folin-phenol reagent. *J Biol Chem* **193**, 265–275.

Mai FD, Chen LY, Ling YC, et al. (2010) Molecular imaging of *in vivo* calcium ion expression in area postrema of total sleep deprived rats: implications for cardiovascular regulation by TOF-SIMS analysis. *Appl Surf Sci* **256**, 4456–4461.

Martino TA, Sole MJ (2009) Molecular time: an often overlooked dimension to cardiovascular disease. *Circ Res* **105**, 1047–1061.

Martino TA, Oudit GY, Herzenberg AM, et al. (2008) Circadian rhythm disorganization produces profound cardiovascular and renal disease in hamsters. *Am J Physiol Regul Integr Comp Physiol* **294**, R1675–R1683.

Mawe GM, Gershon MD (1986) Functional heterogeneity in the myenteric plexus: demonstration using cytochrome oxidase as

a verified cytochemical probe of the activity of individual enteric neurons. *J Comp Neurol* **249**, 381–391.

Meijer JH, Rietveld WJ (1989) Neurophysiology of the suprachiasmatic circadian pacemaker in rodents. *Physiol Rev* **69**, 671–707.

Mendoza J, Challet E (2009) Brain clocks: from the suprachiasmatic nuclei to a cerebral network. *Neuroscientist* **15**, 477–488.

Moore RY (2007) Suprachiasmatic nucleus in sleep-wake regulation. *Sleep Med* **8**, S27–S33.

Nagai K, Nagai N, Shimizu K, et al. (1996) SCN output drives the autonomic nervous system: with special reference to the autonomic function related to the regulation of glucose metabolism. *Prog Brain Res* **111**, 253–272.

Nagaya N, Nishikimi T, Horio T, et al. (1999) Cardiovascular and renal effects of adrenomedullin in rats with heart failure. *Am J Physiol* **276**, R213–R218.

Pennartz CMA, Bierlaagh MA, Geurtsen AMS (1997) Cellular mechanisms underlying spontaneous firing in rat suprachiasmatic nucleus: involvement of a slowly inactivating component of sodium current. *J Neurophysiol* **78**, 1811–1825.

Pennartz CMA, de Jeu MTG, Bos NPA, et al. (2002) Diurnal modulation of pacemaker potentials and calcium current in the mammalian circadian clock. *Nature* **416**, 286–290.

Phillis JW (1992) Na-K ATPase as an effector of synaptic transmission. *Neurochem Int* **20**, 19–22.

Reddy AB, ÓNeill JS (2010) Healthy clocks, healthy body, healthy mind. *Trends Cell Biol* **20**, 36–44.

Reppert SM, Weaver DR (2001) Molecular analysis of mammalian circadian rhythms. *Annu Rev Physiol* **63**, 547–676.

Rüger M, Scheer FA (2009) Effects of circadian disruption on the cardiometabolic system. *Rev Endocr Metab Disord* **10**, 245–260.

Schaap J, Pennartz CM, Meijer JH (2003) Electrophysiology of the circadian pacemaker in mammals. *Chronobiol Int* **20**, 171–188.

Scheer FA, Ter Horst GJ, van Der Vliet J, et al. (2001) Physiological and anatomic evidence for regulation of the heart by suprachiasmatic nucleus in rats. *Am J Physiol Heart Circ Physiol* **280**, H1391–H1399.

Scheer FA, Kalsbeek A, Buijs RM (2003) Cardiovascular control by the suprachiasmatic nucleus: neural and neuroendocrine mechanisms in human and rat. *Biol Chem* **384**, 697–709.

Shaw E, Tofler GH (2009) Circadian rhythm and cardiovascular disease. *Curr Atheroscler Rep* **11**, 289–295.

Smolen AJ (1990) Image analytic techniques for quantification of immuno-histochemical staining in the nervous system. In *Methods in Neuroscience: Quantitative and Qualitative Microscopy*, Vol. 3. (ed. Conn PM), pp. 208–229. San Diego: Academic Press.

Therien AG, Blostein R (2000) Mechanisms of sodium pump regulation. *Am J Physiol Cell Physiol* **279**, C541–C566.

Wang YC, Huang RC (2006) Effects of sodium pump activity on spontaneous firing in neurons of the rat suprachiasmatic nucleus. *J Neurophysiol* **96**, 109–118.

Wong-Riley MTT (1989) Cytochrome oxidase: an endogenous metabolic marker for neuronal activity. *Trends Neurosci* **12**, 94–101.

Yamaguchi S, Isejima H, Matsuo T, et al. (2003) Synchronization of cellular clocks in the suprachiasmatic nucleus. *Science* **302**, 1408–1412.

Yan L (2009) Expression of clock genes in the suprachiasmatic nucleus: effect of environmental lighting conditions. *Rev Endocr Metab Disord* **10**, 301–310.